

Rapid quenching and nitrogenation of $\text{Sm}_2\text{Fe}_{17}$ alloys

J. BLÉTRY, C. TARAVEL, J. P. NOLIN, I. TOUET*, O. SICARDY*

Commissariat à l'Energie Atomique/DTA/CEREM/DEM, *Centre d'Etudes Nucléaires de Grenoble, 85 X, 38041 Grenoble Cedex, France

The production of hard magnetic samarium–iron nitrides by rapid quenching of $\text{Sm}_2\text{Fe}_{17}$ alloys followed by a nitrogenation treatment is described and analysed. Rapid quenching of $\text{Sm}_2\text{Fe}_{17}$ produces almost pure $\text{Sm}_2\text{Fe}_{17}$ phase with 40 to 100 nm grain size. At low temperature ($T \lesssim 465^\circ\text{C}$), the nitrogenation treatment under 1 bar $\text{N}_2\text{-H}_2$ (5%) mainly produces the “definite” compound $\text{Sm}_2\text{Fe}_{17}\text{N}_{3-\delta}$ and follows reasonably well an Arrhenius law, the reaction rate being limited by diffusion through the $\text{Sm}_2\text{Fe}_{17}\text{N}_{3-\delta}$ reacted layer. At higher temperatures ($T \gtrsim 465^\circ\text{C}$), disproportionation reactions simultaneously take place, which transform the metastable nitride into free iron and tiny SmN crystallites (about 10 nm wide). It is concluded that the nitrogenation treatment should be performed at about 400°C in order to reach a sufficient reaction rate for the nitride formation while (possibly) avoiding disproportionation reactions whose by-products (Fe and SmN) are deleterious for permanent magnet applications.

1. Introduction

Samarium iron nitrides, recently discovered by Coey *et al.* [1], are very attractive candidates for permanent magnetic material applications because they combine huge magnetic anisotropy, very large saturation magnetization and high Curie temperature. We therefore intended to produce these compounds by rapid quenching of $\text{Sm}_2\text{Fe}_{17}$ alloys and subsequent nitrogenation treatment in order to obtain finely crystallized nitrides with high magnetic coercivity [2, 3]. The rapid quenching process and the nitrogenation kinetics of $\text{Sm}_2\text{Fe}_{17}$ alloys are described and analysed using mass take-up measurements, X-ray diffraction, scanning electron microscopy and microprobe analysis.

2. $\text{Sm}_2\text{Fe}_{17}$ raw material

Chemical analysis of $\text{Sm}_2\text{Fe}_{17}$ alloy lumps to be quenched showed that their atomic concentration in samarium, $C_{\text{Sm}} = 0.121$, was slightly larger than the expected value: $2/19 = 0.105$. Characterization of these alloys by X-ray diffraction, SEM imaging (back-scattered electrons, atomic number contrast) (Fig. 1) and microprobe analysis, showed three phases:

- (i) the majority 2–17 compound with $\text{Th}_2\text{Zn}_{17}$ hexagonal structure (ASTM 15–431),
- (ii) some free iron (body centred cubic), and
- (iii) some hexagonal Fe_3Sm (ASTM 21–1142).

Traces of eutectic mixture $\text{Fe}_2\text{Sm-Sm}$ could hardly be detected.

3. Rapid quenching $\text{Sm}_2\text{Fe}_{17}$ alloys

3.1. Experimental conditions

Alloy quenching experiments were performed by the

melt-spinning technique. The alloys were melted by r.f. heating at about 1430°C into boron nitride crucibles (BN-coated graphite crucibles gave almost pure SmC_2 quenched ribbons). Samarium–iron molten alloys were ejected through a 1 mm wide boron nitride nozzle under a 400 mbar excess pressure. A 100 mbar helium pressure was set up in the quenching vessel in order to restrict samarium evaporation and to avoid oxidation of the alloy.

The alloy jet was quenched on to a copper wheel rotating at 2000 r.p.m. (40 m s^{-1} peripheral speed) and the sticking length between the alloy and the wheel was about 1 cm. The quenched alloy ribbons were between 10 and 20 μm thick, and due to their brittleness, fell into pieces or “flakes” during retrieval operations.

3.2. As-quenched $\text{Sm}_2\text{Fe}_{17}$ alloys

The samarium concentration of the quenched alloy, measured by chemical analysis, was found to be 9.0 at %, indicating a 3.1% samarium loss during quenching operations.

X-ray diffraction patterns of these alloys (Fig. 2) show that they are made from almost pure $\text{Sm}_2\text{Fe}_{17}$ phase, together with some free iron traces.

The grain size, G , of quenched alloys was estimated from SEM images (Fig. 2) to range between 50 and 100 nm. Calculation of G from the widening of diffraction lines according to the Scherrer relation

$$G = \frac{0.9\lambda}{\Delta_{1/2}(\theta) \cos \theta_{hkl}} \quad (1)$$

(where λ is the X-ray wavelength ($\lambda_{\text{Co}} = 0.179 \text{ nm}$), θ_{hkl} the Bragg angle of the hkl line, and $\Delta_{1/2}(\theta)$ the

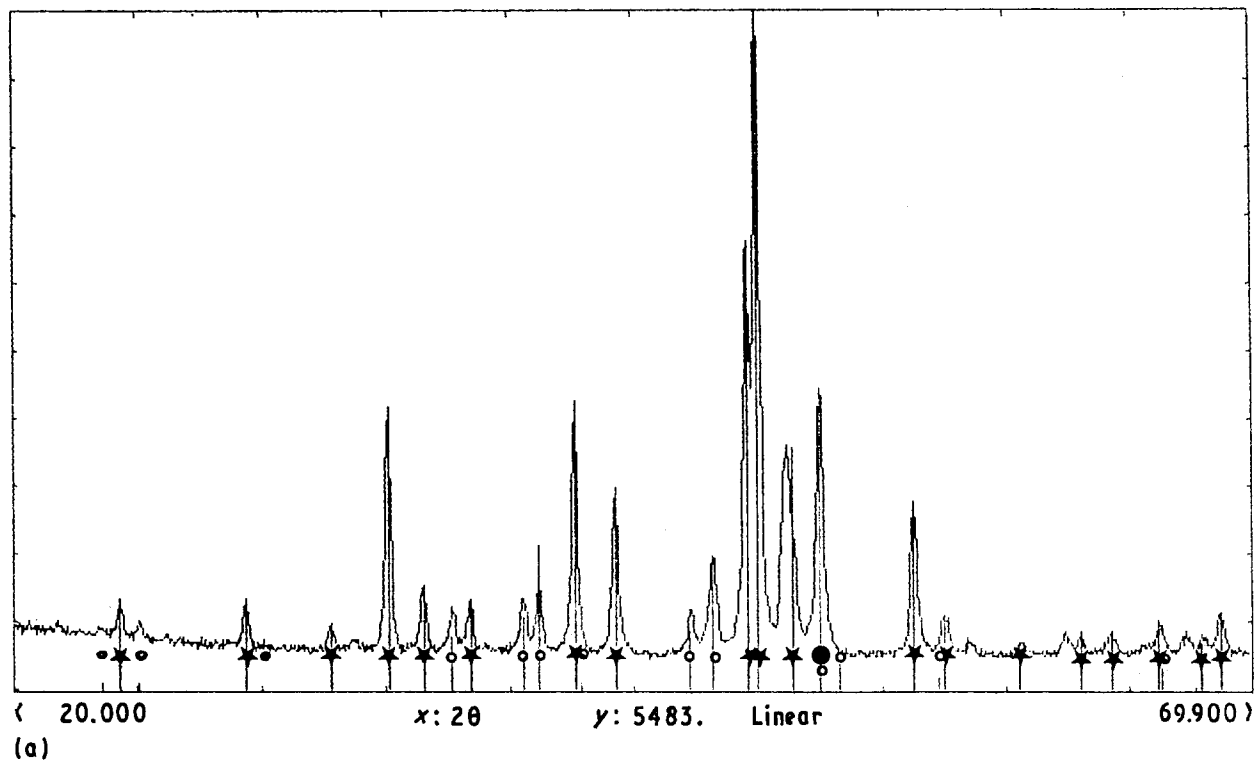
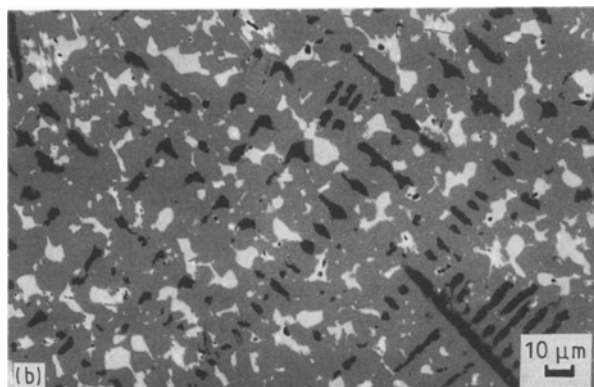


Figure 1 (a) X-ray diffraction pattern ● Fe; ★ $\text{Sm}_2\text{Fe}_{17}$; ○ SmFe_3 and (b) backscattered electron image (\bar{Z} contrast) of $\text{Sm}_2\text{Fe}_{17}$ alloys.



variations, $\Delta m/m$, were of the order of 1% (Table I). If one excludes short reaction times, where experimental accuracy is poor, isothermal mass take-up follows a $t^{1/2}$ time variation law (Fig. 3) reasonably well. Furthermore, reaction times corresponding to a given mass take-up at different temperatures fulfil with good accuracy the Arrhenius law

$$t = t_0 \exp\left(-\frac{E}{kT}\right) \quad (2)$$

where $E = 0.81$ eV of $E/k = 9396^\circ\text{C}$ is the activation energy given by Coey *et al.* [1], and t_0 is a constant time.

All these results are in agreement with the following nitrogenation mechanism. The reaction between solid $\text{Sm}_2\text{Fe}_{17}$ and nitrogen gas proceeds through the insertion of N^{2-} anions into octahedral interstitial sites of $\text{Sm}_2\text{Fe}_{17}$ and the reaction rate is limited by the diffusion speed of these anions through the $\text{Sm}_2\text{Fe}_{17}\text{N}_x$ reacted layer which forms at the expense of $\text{Sm}_2\text{Fe}_{17}$ grains [4]. MEB observations by Schrey and Rodewald at Vacuumschmelze GmbH [5] confirm the existence of this reacted $\text{Sm}_2\text{Fe}_{17}\text{N}_x$ layer around unreacted $\text{Sm}_2\text{Fe}_{17}$ grains.

Finally, if one assumes that most of the mass taken up is due to the formation of this $\text{Sm}_2\text{Fe}_{17}\text{N}_x$ compound, the maximum value of x can be estimated for long reaction times i.e. when the reaction is completed. At $T = 465^\circ\text{C}$ one finds $x = 3 - \delta = 2.7$, which is a quite plausible value, because the $\text{Sm}_2\text{Fe}_{17}$ lattice cell offers three octahedral insertion sites to N^{2-} anions [6]. However, the more detailed reaction analysis presented below shows that the nitrogenation process is more complex than this simple description, because disproportionation reactions (which are slow and

width at half maximum of this hkl line), confirmed this order of magnitude.

4. Nitrogenation of $\text{Sm}_2\text{Fe}_{17}$ quenched alloys

4.1. Experimental conditions

The nitrogenation kinetics of the quenched alloys were studied at three temperatures: $T = 465, 535$ and 630°C using reactive treatments performed under a 1 bar pressure of $\text{N}_2\text{-H}_2$ (5%) gas mixture and for durations ranging between 15 and 8000 min. 5 at% hydrogen was introduced into the nitrogenating atmosphere in order to avoid alloy oxidation. Minimum reaction times were limited to 15 min because of the rise-time required by the alloy to reach the chosen reaction temperature.

4.2. Mass take-up measurements and analysis of the nitrogen-insertion process

The reaction kinetics was first followed by measuring the time variations of the alloy mass during nitrogenation at three different temperatures. Relative mass

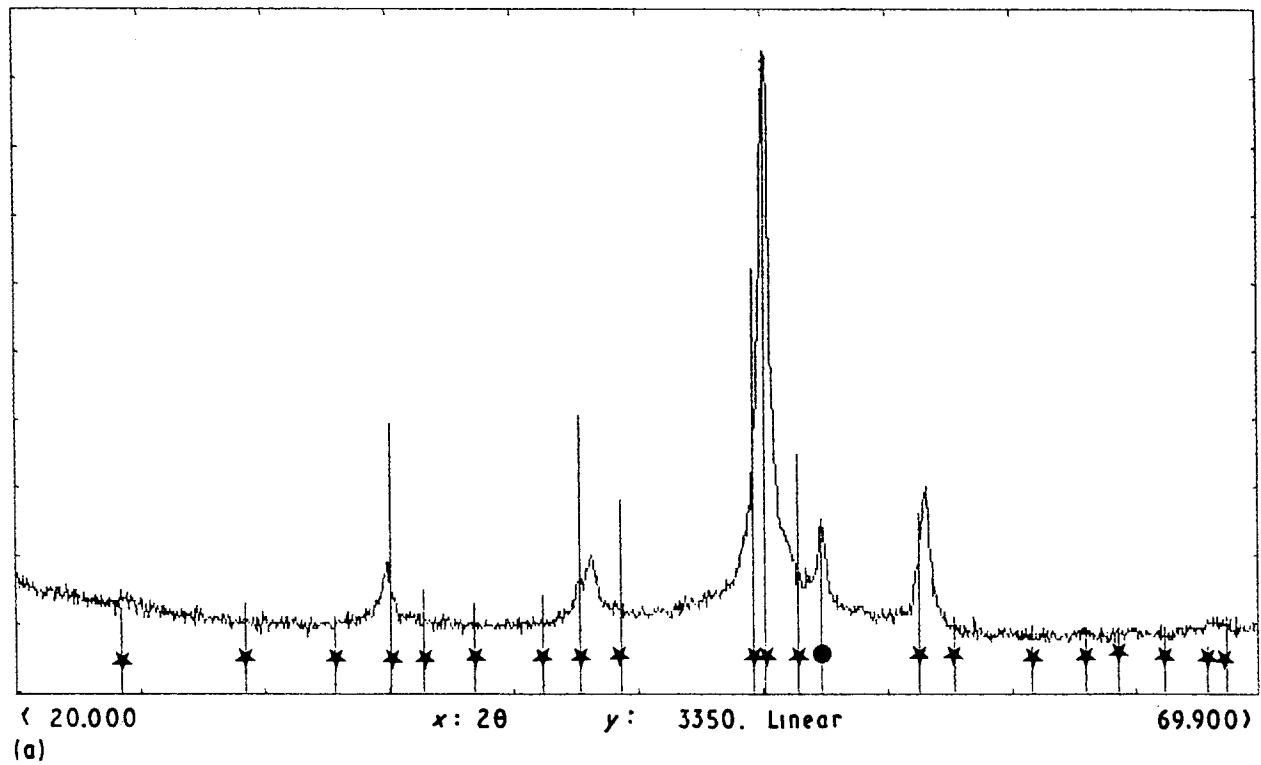
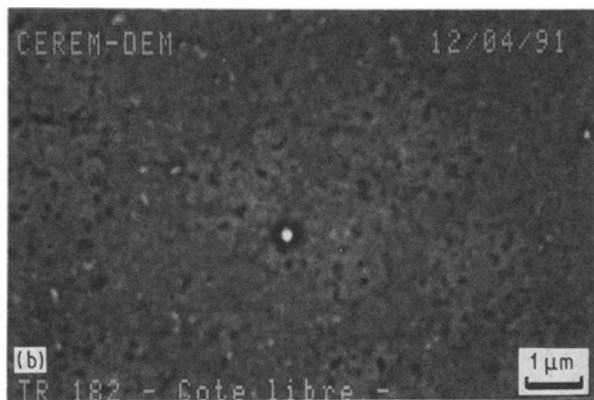


Figure 2 (a) X-ray diffraction pattern ★ $\text{Sm}_2\text{Fe}_{17}$; ● Fe and (b) backscattered electron image (\bar{Z} contrast) of rapidly quenched $\text{Sm}_2\text{Fe}_{17}$ alloys.



(a) the virgin $\text{Sm}_2\text{Fe}_{17}$ phase with hexagonal lattice parameters $a = 0.8536 \text{ nm}$ and $c = 1.2429 \text{ nm}$ [1], and

(b) the nitrogenated compound $\text{Sm}_2\text{Fe}_{17}\text{N}_x$, with an expansion in the hexagonal lattice parameters a and c of the order of

$$\frac{\Delta a}{a} \simeq \frac{\Delta c}{c} \simeq \frac{\Delta \theta_{hkl}}{\text{tg } \theta_{hkl}} = 1.5\% \quad (3)$$

In the last nitrogen insertion stage, the lines of the $\text{Sm}_2\text{Fe}_{17}\text{N}_x$ compound remain alone and shift slightly towards smaller scattering angles indicating a weak nitrogen take-up of this nitride.

could possibly be neglected at 465°C) simultaneously take place with the insertion reaction.

4.3. X-ray diffraction and phase analysis of the nitrogenation process: nitrogen insertion versus disproportionation

The nitrogenation process of $\text{Sm}_2\text{Fe}_{17}$ quenched alloys was further interpreted by analysing the X-ray scattering patterns of these alloys after nitrogenation treatments with variable duration performed at three different temperatures. Fig. 4 shows the overall scattering patterns of these alloys and Fig. 5 is a zoom over their more intense diffraction lines.

4.3.1. Nitrogen insertion

During the first (shortest) nitrogenation step, shoulders appear on all the diffraction lines of the $\text{Sm}_2\text{Fe}_{17}$ phase at smaller scattering angles. Pursuing the nitrogenation treatment further, all the $\text{Sm}_2\text{Fe}_{17}$ lines split into two lines with almost constant separation. These lines respectively correspond to:

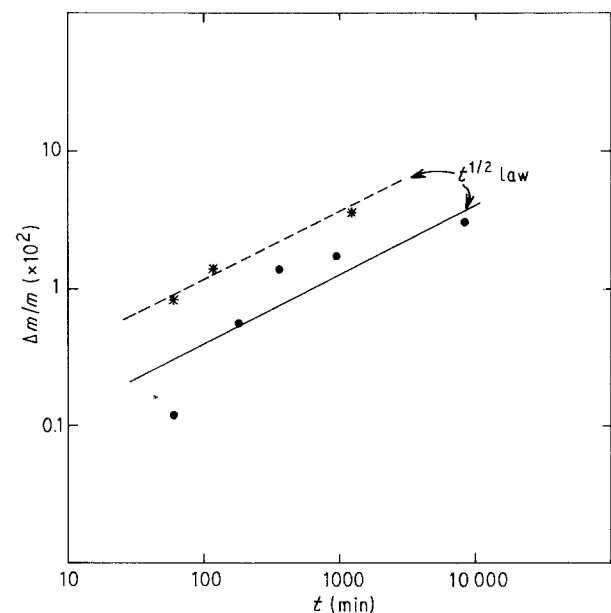
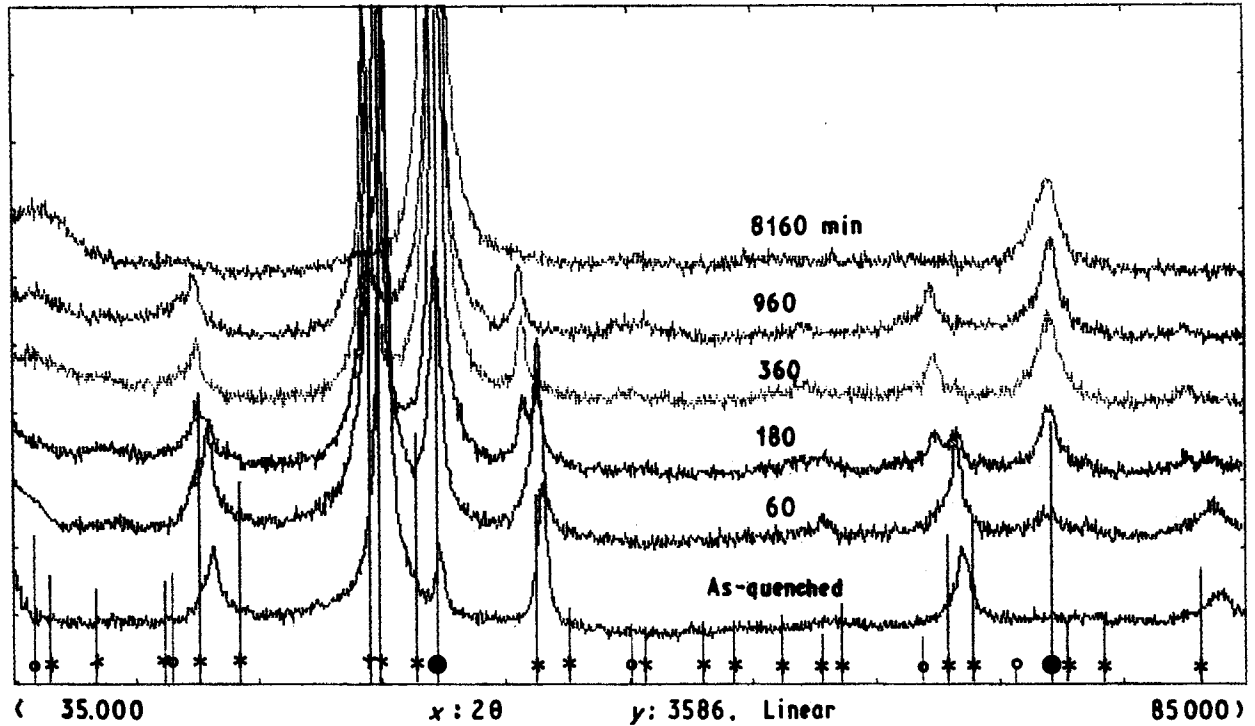


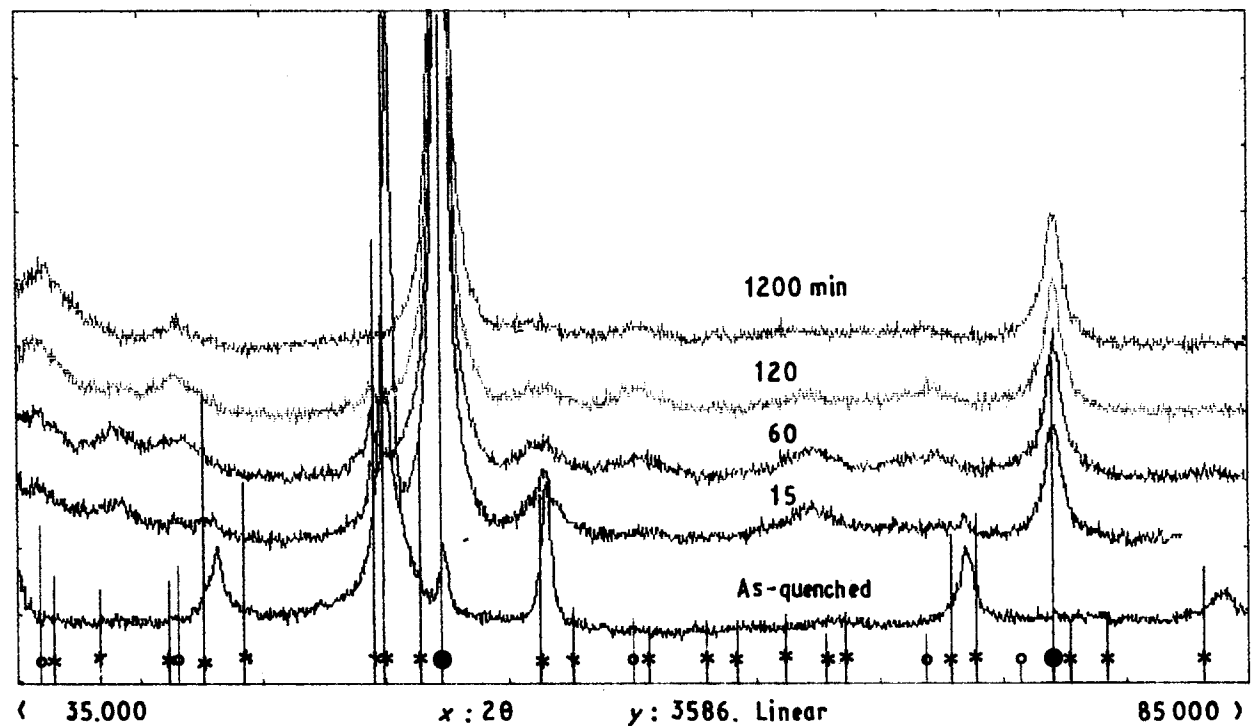
Figure 3 Kinetics of the mass take-up of $\text{Sm}_2\text{Fe}_{17}$ alloys during isothermal nitrogenation treatments. $T = (\bullet) 738 \text{ K}$, $(*) 808 \text{ K}$.

TABLE I Time variations of the relative mass taken up, $\Delta m/m$ (%), of $\text{Sm}_2\text{Fe}_{17}$ quenched alloys during their nitrogenation

Temperature (°C)	Time (min)							
	15	60	120	180	360	960	1200	8160
465	0.02	0.12		0.56	1.4	1.7		3.04
535	0.85	0.82	1.4				2.6	
630	1.4							



(a)



(b)

Figure 4 Evolution of the X-ray diffraction patterns of $\text{Sm}_2\text{Fe}_{17}$ alloys during isothermal nitrogenation treatments at $T =$ (a) 465 °C and (b) 535 °C. ● Fe; * $\text{Sm}_2\text{Fe}_{17}$; ○ SmN.

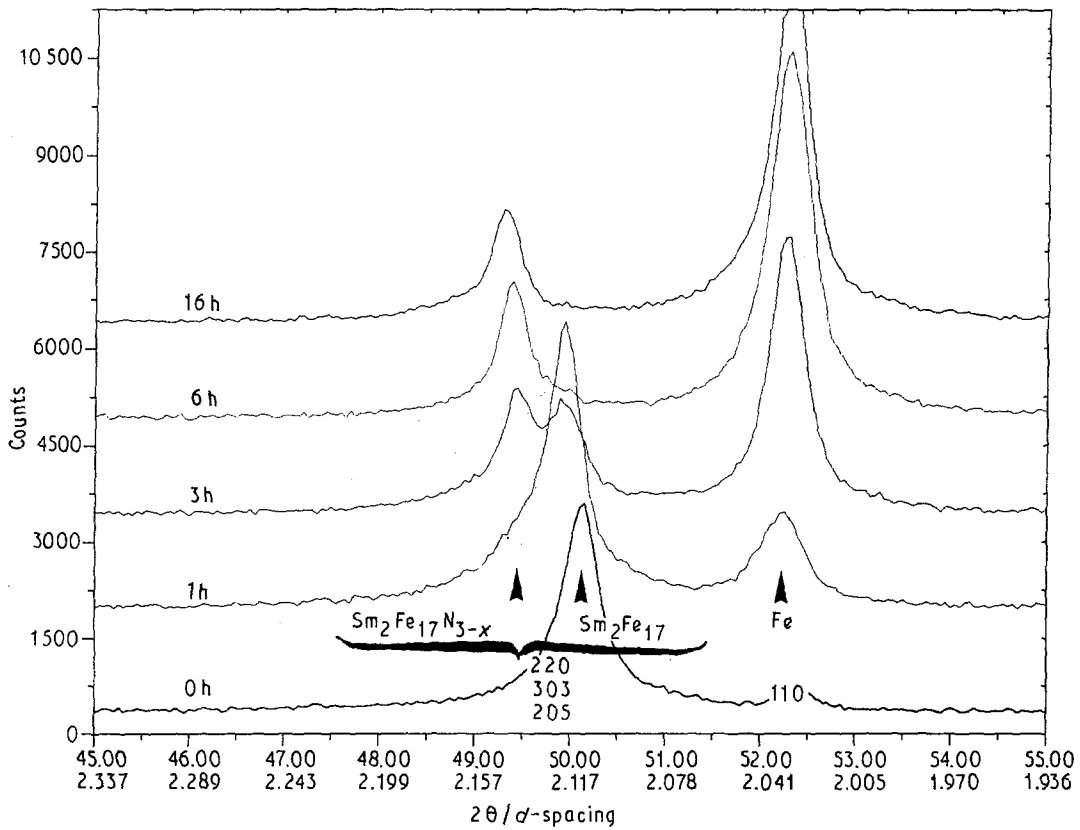


Figure 5 Evolution of the X-ray diffraction main lines of $\text{Sm}_2\text{Fe}_{17}$ alloys during nitrogenation at $T = 465^\circ\text{C}$.

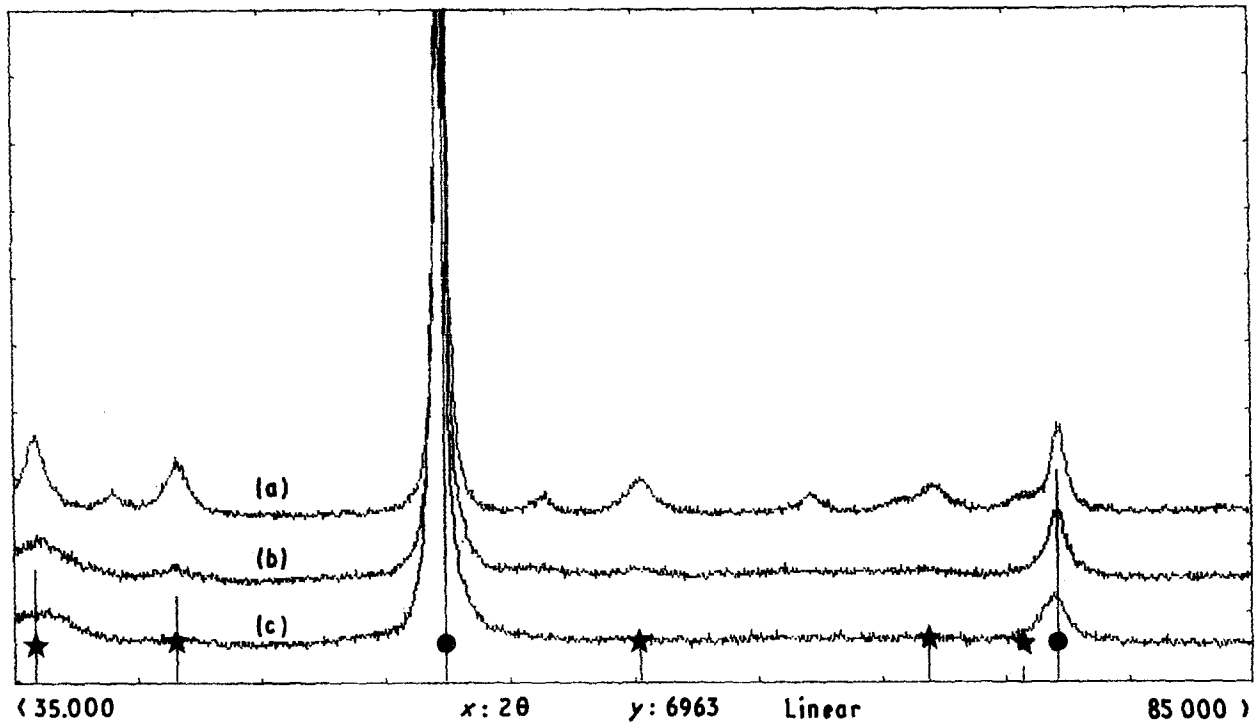


Figure 6 X-ray diffraction patterns of disproportionated $\text{Sm}_2\text{Fe}_{17}\text{N}_x$ alloys after (a) 60 min at $T = 630^\circ\text{C}$, (b) 1200 min at $T = 535^\circ\text{C}$, (c) 8160 min at $T = 465^\circ\text{C}$, nitrogenation times. ● Fe; ★ SmN.

All the results in Sections 4.2 and 4.3 show that the $\text{Sm}_2\text{Fe}_{17}\text{N}_x$ phase is an almost definite compound with stoichiometry close to $x \approx 3$.

Finally, it must be noted that the width of $\text{Sm}_2\text{Fe}_{17}$ and $\text{Sm}_2\text{Fe}_{17}\text{N}_x$ diffraction lines remains constant during the whole nitrogenation treatment, showing that no grain growth takes place during the insertion reaction.

4.3.2. Disproportionation reactions

Simultaneously with the splitting of $\text{Sm}_2\text{Fe}_{17}$ lines, which comes from the nitrogen insertion reaction, the intensity of free iron diffraction lines increases (Fig. 5) and new weak “bumps” appear in the scattering pattern, which transform into very wide lines with increasing nitrogenation time (Figs 4 and 6). These new lines correspond to the cubic SmN phase (ASTM

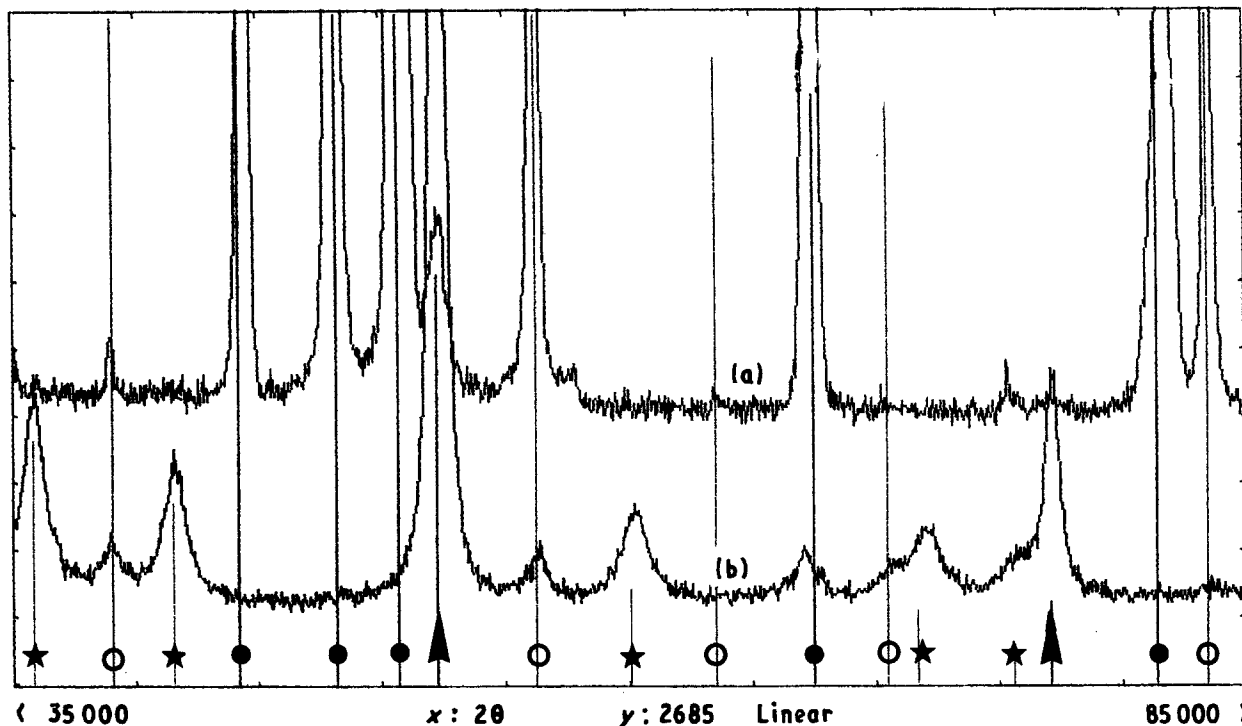


Figure 7 Comparison between the X-ray diffraction patterns of (a) CERAC iron nitride powder, and (b) fully disproportionated $\text{Sm}_2\text{Fe}_{17}\text{N}_x$ alloys (60 min at $T = 630^\circ\text{C}$). \blacktriangle Fe; \bullet Fe_3N ; \square Fe_4N ; \star SmN.

30–1104) and, due to their large width and to their weakness, may have been disregarded by other authors.

In fact, the size of SmN grains estimated from the broadening of diffraction lines by Equation 1 ranges between 10 and 20 nm, after a 1200 min nitrogenation time at 535°C , and they could not be observed by SEM imaging.

Finally, in the last nitrogenation step, $\text{Sm}_2\text{Fe}_{17}\text{N}_x$ lines disappear indicating a complete disproportionation of this compound into Fe, SmN and even iron nitrides Fe_3N and Fe_4N (see Fig. 7 where comparison is made between the scattering pattern of fully disproportionated alloys and CERAC iron nitride powder).

All these results, show that disproportionation reactions take place simultaneously with the interesting nitrogen-insertion reaction, although their reaction rates are slow at the lowest temperature studied (465°C).

5. Conclusion

It is shown that it is possible to prepare the $\text{Sm}_2\text{Fe}_{17}\text{N}_x$ insertion compound, with $x \approx 2.7$ and a grain size ranging between 50 and 100 nm, by rapid quenching of $\text{Sm}_2\text{Fe}_{17}$ alloys and subsequent nitrogenation treatment. However, a disproportionation process simultaneously takes place, which transforms the metastable $\text{Sm}_2\text{Fe}_{17}\text{N}_x$ compound into Fe and SmN phases and is first detected by the increase of

iron diffraction lines in the X-ray scattering pattern. In order to avoid this disproportionation process, which is very deleterious for the use of $\text{Sm}_2\text{Fe}_{17}\text{N}_x$ as permanent magnetic material, one should therefore perform the nitrogenation treatment at low but sufficient temperature ($T \approx 400^\circ\text{C}$), in order to achieve a reasonable nitrogen insertion rate.

Acknowledgement

This work was sponsored by the CEC as part of an EURAM advanced material programme MAIE/0073/C (CD).

References

1. J. M. D. COEY, HU BOPING, D. P. F. HURLEY, LI HONGSHUO, Y. OTANI and SUN HONG, CEAM 2 Final report, Villars de Lans (France), 24–25 May 1991.
2. S. PAIDASSI, J. BLETRY, W. RODEWALD and P. ROGL 4th Technical Report, EURAM Project MAIE/0073/C(CD) (1990).
3. BLETRY, W. RODEWALD and P. ROGL, 5th Technical Report, EURAM Project MAIE/0073/C(CD) (1990).
4. P. BARRET, "Cinétique hétérogène" (Gauthier, Villars, 1973).
5. P. SCHREY and W. RODEWALD, private communication, 1991.
6. D. FRUCHART, O. ISNARD, S. MIRAGLIA, S. OBADE, L. PONTONNIER, J. L. SOUBEYROUX and P. WOLFERS, CEAM 2, Final Report, Villars-de-Lans, France, 24–25 May 1991.

Received 7 October
and accepted 25 November 1991